Vol. 22, n.° 2, julio-diciembre de 2024
ISSN impreso: 1657-6527 • ISSN en línea: 2145-8502

FUENTES
EL REVENTÓN ENERGÉTICO

DETERMINATION OF HYDRODYNAMIC AND THERMAL PROFILES WITHIN A PYROLYTIC REACTOR LOADED WITH PALM SHELL USING COMPUTATIONAL FLUID DYNAMICS

DETERMINACIÓN DE PERFILES HIDRODINÁMICOS Y TÉRMICOS DENTRO DE UN REACTOR PIROLÍTICO CARGADO CON CÁSCARA DE PALMA UTILIZANDO DINÁMICA DE FLUIDOS COMPUTACIONAL

Mariapaz Moreno-Pinilla, Joan Sebastián Rueda-Castiblanco, Harvey Andrés Milquez-Sanabria*, Jaime Eduardo Arturo-Calvache

Semillero SIM PRO – Grupo de Investigación GPS, Facultad de Ingenierías. Universidad de América, Bogotá, Av- Circunvalar # 20 -53, Colombia.

mariapaz.moreno@estudiantes.uamerica.edu.co, joan.rueda@estudiantes.uamerica.edu.co, harvey.milquez@profesores.uamerica.edu.co*, jaime.arturo@profesores.uamerica.edu.co

Recibido: 11 de marzo de 2024. Aprobado: 21 de agosto de 2024. Versión final: 9 de octubre de 2024.

Highlights

- CFD simulation as a tool to visualize and adjust parameters in pyrolysis.
- Phenomena of mass, heat and momentum transfer integrated intro the modeling.
- Palm kernel as biomass for pyrolysis in fixed bed reactor.
- Alternate source of energy by obtaining tar.

Abstract

In this research, the modeling and simulation of a laboratory-scale pyrolytic reactor with tubular geometry loaded with palm kernel was carried out using the COMSOL Multiphysics® V5.6 software; For the modeling, the physicochemical properties from the palm shell found in different bibliographic sources were used, as well as the initial flow conditions and concentrations to estimate hydrodynamic, thermal and kinetic profiles present in the absorption of the biomass entered in the fixed bed, contemplating isothermal and non-isothermal conditions. The results indicate that the formation of tar is favored at a temperature of 723.15 to 773.15 K, with a reaction time of 10 to 12 min and the relationship of the geometry change with respect to the thermal and hydrodynamic profiles, these are in accordance with the references consulted and can be used as a starting point for future research to understand the phenomena presented within a pyrolysis reactor.

Keywords: Thermochemical treatment; Biomass; Reactor; Porous medium; COMSOL.

Cómo citar: Moreno-Pinilla, M., Rueda-Castiblanco, J. S., Milquez-Sanabria, H. A. & Arturo-Calvache, J. E. (2024). Determination of hydrodynamic and thermal profiles within a pyrolytic reactor loaded with palm shell using computational fluid dynamics. *Fuentes, El Reventón Energético*, *22*(2), 19-34.
https://doi.org/10.18273/revfue.v22n2-2024002

Resumen

En esta investigación se realizó el modelamiento y simulación de un reactor pirolítico a escala de laboratorio con geometría tubular cargado con palmiste, utilizando el software COMSOL Multiphysics® V5.6; para el modelamiento se utilizaron las propiedades fisicoquímicas de la cáscara de palma encontradas en diferentes fuentes bibliográficas, así como las condiciones iniciales de flujo y concentraciones para estimar los perfiles hidrodinámicos, térmicos y cinéticos presentes en la absorción de la biomasa ingresada en el lecho fijo, contemplando condiciones isotérmicas y no isotérmicas. Los resultados indican que la formación de alquitrán se favorece a una temperatura de 723,15 a 773,15 K, con un tiempo de reacción de 10 a 12 min y la relación del cambio de geometría respecto a los perfiles térmicos e hidrodinámicos, estos concuerdan con las referencias consultadas y pueden ser utilizados como punto de partida para futuras investigaciones para comprender los fenómenos presentados dentro de un reactor de pirólisis.

Palabras clave: Tratamiento termoquímico; Biomasa; Reactor; Medio poroso; COMSOL.

1. INTRODUCTION

Colombia is the fourth producer of palm oil in the world and the first in America (Fedepalma, 2021) where the national production presented an increase of 2 % reaching 1.56 million tons of oil produced in 2020 according to data reported by FEDEPALMA. One hectare planted with palm produces up to 10 times more oil than other species, classifying it as one of the most productive oil plants on the planet (Reyes-Rodriguez et al., 2019). To carry out the extraction of palm oil, the process begins with the separation of the empty clusters, continuing with the cold pressing to obtain the product of interest, at this stage solid waste is available; bagasse together with palm kernels produces approximately 3 Mt/year of agricultural residual biomass in Colombia, where 20 % of the bunch weight represents the extracted oil and 80 % equivalent to the remaining value belongs to the aforementioned waste (Anaya-Aldana and Molina-Crespo, 2018).

The use of residual biomass through pyrolysis is an alternative for obtaining sustainable energy sources (Verdeza-Villalobos et al., 2019; Ayala-Ruíz et al., 2022). Since the palm kernel contains lignin in a higher percentage (44 – 50 %), causing the liquid product to be rich in phenols, serving as biofuels and raw material to produce various value-added products in the cosmetic and food industries (Basu, 2018; Ministry for ecological transition, 2020). It should also be noted that it is a by-product released in the operation of the profit plants where 0.13- 0.4 tons (per ton of crude oil) are obtained at cost (Van-Dam J, 2016) and has an energy potential of 2677.44 TJ/year (Okoye et al., 2018).

Different studies have been carried out, which leads to the use of specific software and hardware for the analysis of the processes in which the biomass is treated using commercial simulators such as Aspen (Pauls et al., 2016; Ramanathan et al., 2022; Castiblanco-Urrego and Milquez-Sanabria, 2021) among others, based on kinetic pathways (reaction rates and activity), thermodynamic pathways (phase balances and energy balances) that simulate the reactor and its outlet currents according to input and operating conditions. However, it is observed that there are adverse effects that are not considered, such as the transfer of mass and heat present in the particles, as well as the fluid regime inside the reactor. Due to these phenomena, the solution of complex systems must be examined using numerical methods and progressively continue with simulators in charge of predicting the variables needed, being studied by the Computational Fluid Dynamics (CFD). Until now, the studies carried out in previous years were based on the experimentation of thermochemical processes; gasification (Liu et al., 2017) and pyrolysis (Okoye et al., 2018) within reactors fed by residual agricultural biomass from the palm industry, presenting the drawbacks.

The objective of this study is to determine hydrodynamic and thermal profiles within a fixed-bed pyrolytic reactor loaded with palm kernels by using CFD as a method to understand the transport phenomena that occur in the reactor design; taking into account the kinetics and reaction velocity present in the decomposition of cellulose, hemicellulose and lignin in the palm kernel, compare the products obtained inside the reactor with experimental data found in the literature accompanied by temperature profiles obtained by the program to be used.

2. MATERIALS AND METHODS

2.1. Validation of the mathematical model

For the mathematical modeling together with the development, learning and coupling of the program to be used, a case study developed and published by Wijayanti et al. (2021) was previously carried out, where they modeled a pyrolysis reactor using mahogany wood as a packed bed and the comparison of the results with a pilot plant, for the process a heating rate of 1073 K/h was maintained by coupling physical interfaces for porous media for heat transfer and movement of the dragging fluid (nitrogen). This case study was replicated, obtaining results consistent with those described in the article.

2.2. Suppositions

In the modelling of the pyrolysis process, the reactor loaded with palm shells, the following assumptions were made based on those implemented by Wijayanti et al. (2021), Solanki et al. (2022), Thoharudin et al. (2020) and Sechage-Cortés et al. (2017).

- Uniform heat rates are considered limiting the boundary conditions by decreasing the computational density of the model.
- Flow in laminar state without the presence of turbulence in the pores due to the low nitrogen velocity, which can be covered with a Darcian flow model that defines a linear relationship.
- A low production of non-condensable gases was considered due to the high temperature of the process and its reaction time so a reversible production of tar to non-condensable gases will not be considered.
- Pulverized and dried palm kernel oil, the interaction of the mathematical model is not considered and there is no drying step along the process.
- The material properties and transfer coefficient are constants at different temperatures that influence the mathematical model obtaining results in an accurate range.

2.3. Biomass used: Palm shell

The waste chosen for the process was the palm shell, which is the main waste after the extraction of oil from the oleaginous fruit from the extraction of palm kernel oil. Biomass is modelled as an unconventional solid component which that not available in the program's database (COMSOL Multiphysics). For that reason, it is required to enter the characteristic properties of the material.

Table 1 presents the data chosen to be added to the software based on a previous compilation of values reported in the literature by different authors (Sechage -Cortés et al., 2017; Chang et al., 2016; Hussain et al., 2022; Tripathi et al., 2016; Abdullah et al., 2015) being the last one the reference with all the complete data within the ranges proposed by the other sources, it should be noted that according to the methodology to be followed, the organic components were of the utmost importance for the modelling of the reactor.

Table 1. Palm shell characterization.

		Palm shell characterization (Abdullah et al., 2015)
Organic components %	**Cellulose**	28.03
	Hemicellulose	20.69
	Lignin	43.08
Elemental Analysis %	**C**	46.59
	H	5.56
	N	0.27
	O	47.28
	S	0.16
Analysis Next %	**Humidity**	11
	Volatile	67.2
	Ash	2.1
Calorific value MJ/kg		19.10

Table 2 refers to the physical properties of the palm shell, entering the average of the values found by different authors, in addition to the data reported the following was considered: permeability from 2.6exp-12 m^2 (Wijayanti et al., 2021).

Table 2. Physical properties of the palm kernel.

Parameters	Nomenclature	Units	(Asadullah et al., 2013)	(Koya et al., 2013)	(Ezeoha et al., 2012)	Average
Apparent density	r_a	kg/m^3	773	560	711	681
Heat capacity	Cp	J/kg*K	2220	1983	4130	2778
Thermal conductivity	λ	w/m*K	NR	0.68	NR	0.68
Porosity	ε	NR	0.13	NR	NR	0.13

NR: Not reported.

2.4. Scheme Reactions in the system

Cellulose, hemicellulose, and lignin are transformed into active biomass and, being in contact with the hot wall of the reactor and the fluid, break down into tar, coal and non-condensable gases, secondary cracking will not be taken into account due to the low production of these gases can be evidenced in figure 1 where a general scheme describes what happened with each component of the biomass to be treated and their respective reaction rates, the term Y refers to the percentage of the final product corresponding to biochar, the remaining will be non-condensable gases.

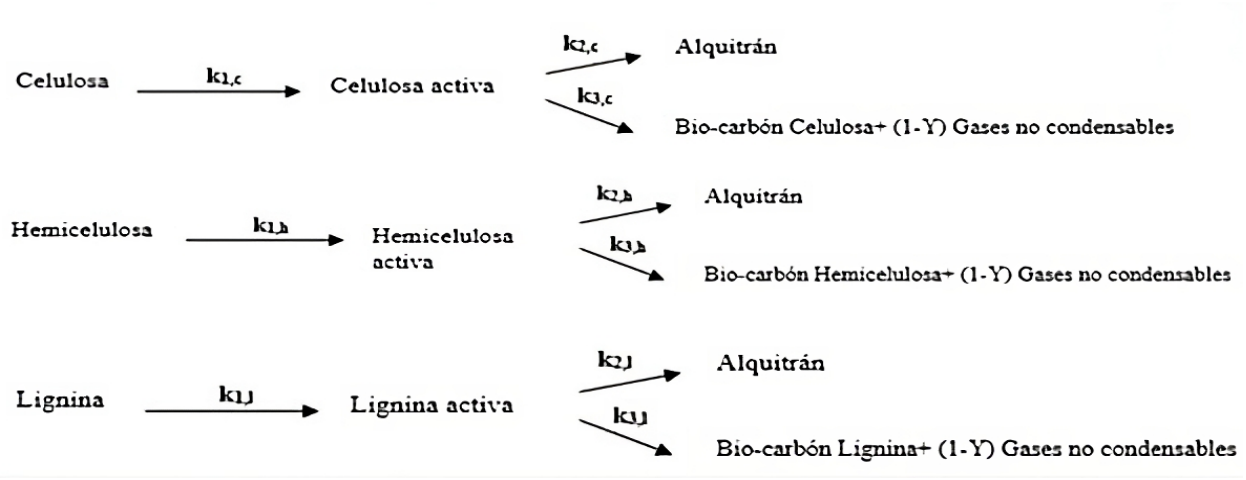

Figure 1. General scheme of Cellulose, Hemicellulose and Lignin reactions.
Note : Own elaboration adapted from Thoharudin et al. (2020).

2.5. Reaction Kinetics

According to the general scheme of reactions represented in Figure 1, table 3 is a compilation of the values referring to the Arrhenius equation (1) for each reaction.

$$k_i(T) = A_i\ exp\ (-E_{ai}/RT) \quad (1)$$

Table 3. Kinetic parameters and enthalpy change of biomass pyrolysis.

Reaction	Y	A (s^{-1})	E_{ai} (kJ/kmol)	∆h (kJ/kg)
k1,c		2.80E+19	242.4	0
k2,c		3.28E+14	196.5	255
k3,c	0.35	1.30E+10	150.5	-20
k1,h		2.10E+16	186.7	0
k2,h		8.75E+15	202.4	255
k3,h	0.6	2.60E+11	145.7	-20
k1,l		9.60E+08	107.6	0
k2,l		1.50E+09	143.8	255
k3,l	0.75	7.70E+06	111.4	-20

Note: Own elaboration adapted from Thoharudin et al. (2020) and Liu et al. (2017).

2.5.1. Validation of the kinetic model

The kinetics proposed by Thoharudin et al. (2020). were previously elaborated by a series of collection of kinetic parameters described by Liu et al. (2017). that represent the decomposition of hemicellulose, cellulose, and lignin as a reactive process in series where due to the thermal effect the biomass presents an opening of the pore becoming active biomass and finally a reactive process in parallel carrying out the degradation of said biomass into tar and coal together with secondary cracking for the formation of gases from the tar. For the present case of study, said first order kinetic model was previously analysed in the COMSOL Multiphysics program with the conditions presented by Kim et al. (2010). where a fluidized bed reactor was operated in order to obtain the best conditions for obtaining tar in the which highlights an operating temperature of 491 °C and their respective yields, when checking the graphic results it is observed that at said temperature a yield of 48.7 %wt is obtained for the production of tar and 55.1 %wt of yield under the simulation of the kinetics, which corresponds to a 7.3 % margin of error for tar production, which indicates that there would be a variation in performance but that the simulated results mare close to those expected in a laboratory-scale reactor.

2.6. Operating conditions

The dimensions of the equipment were those of an oven with a fixed-bed tubular system measuring 102 cm long and with an internal diameter of 1.5 cm, this was loaded with 30 g of palm kernel and pyrolysis occurs at a rate of oven heating at 30 K/min with nitrogen gas input at a rate of 30 mL/min as reported by Yakub et al. (2015a).

Figure 2 shows the currents of mass and energy, the red arrows indicate the heat supplied to the walls of the bed from the tubular furnace, which will be thermally insulated to prevent heat loss, the nitrogen flow will enter on the left side (Blue line) and on the right side will be the output of the products of the pyrolysis process (Black line).

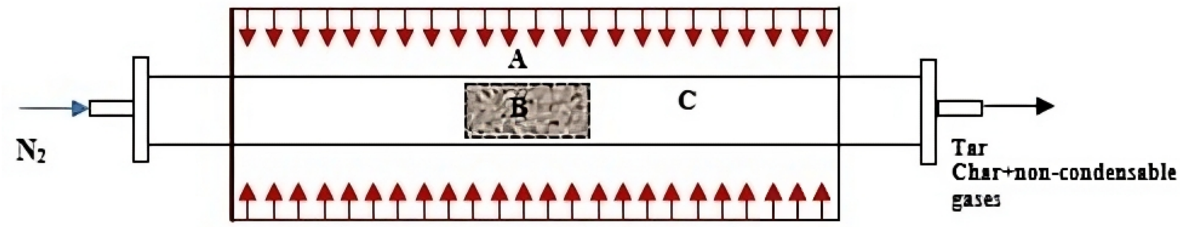

Figure 2. (A) Tube Furnace, (B) Packed Bed, (C) Alumina Tube.
Note: Own elaboration adapted from Yakub et al. (2015b).

Modelling

The modeling was carried out in 2 temporary spaces using the COMSOL MULTIPHYSICS software:

1. Kinetic modeling determining the reaction rate as a function of time and temperature.

2. Thermal modeling to determine the temperature profiles and velocity modeling with pressure throughout the reactor

For the transfer of heat and present moment inside the pyrolytic reactor, the following equations were used:

1. Heat transfer in porous media

It was selected to model heat transfer by conduction and convection in porous media, in the domains the temperature equation corresponds to the convection-diffusion equation, on the other hand, with the heat phenomena, the biomass temperature during pyrolysis can be known. Likewise, during the first phase, the heating rate participates and continues with the diffusivity to decompose the biomass, which is mainly composed of hemicellulose, cellulose, and lignin.

The equations that describe the energy transfer in the fixed bed reactor are:

$$d_z(\rho C_p)_{eff}\frac{\partial T}{\partial t} + d_z\rho_f C_{p,f} u\nabla T + \nabla q = d_z Q + d_z Q_{vd} + q_0 + d_z Q_p + d_z Q_{geo} \quad (2)$$

$$q = -d_z K_{eff}\nabla T \quad (3)$$

$$(\rho C_p)_{eff} = \epsilon_p\rho_f C_{p,f} + \theta_s\rho_s C_{p,s} + \theta_{imf}\rho_{imf}C_{p,imf} \quad (4)$$

$$\frac{1}{K_{eff}-K_{disp}} = \frac{\epsilon_p}{K_f} + \frac{\theta_s}{K_s} + \frac{\theta_{imf}}{K_{imf}} \quad (5)$$

$$K_s = \frac{K_b}{\theta_s}, \rho_s = \frac{\rho_b}{\theta_s}, C_{p,s} = \frac{Cp_b}{\theta_s} \quad (6)$$

In Equations 3-6, a mixing rule is applied to find the effective thermal conductivity and the effective heat capacity from the porosity and the amount of immobile fluid, which are solved simultaneously.

$$-n \cdot q = \varepsilon\sigma(T_{amb}^4 - T2^4) \tag{7}$$

This study takes into account the effect of heat transfer by radiation (7) from the outer wall of the oven to the environment with emissivity value 1, likewise the oven will be thermally insulated to prevent heat loss.

2. Brinkman equations.

This approach determines the velocity and pressure fields for single-phase flow in porous media under laminar conditions. By extending Darcy's law, the physical model accounts for the dissipation of kinetic energy caused by viscous shear (Solanki et al., 2022).

The equations formed from the continuity and momentum equations are:

$$\frac{1}{\epsilon_p}\rho\frac{\partial u}{\partial t} + \frac{1}{\epsilon_p}\rho(u \cdot \nabla)u \ \frac{1}{\epsilon_p} = \nabla \cdot [-pI + K] - \left(\mu K^{-1} + \beta\rho|u| + \frac{Q_m}{\epsilon_p^2}\right)u + F \tag{8}$$

In equation 8, the parameters of viscosity, permeability and flow rate for the fluid phase and the porous matrix will be resolved.

$$\frac{\partial \epsilon_p \rho}{\partial t} + \nabla \cdot (\rho u) = Q_m \tag{9}$$

$$K = \mu\frac{1}{\epsilon_p}(\nabla u + (\nabla u)^T) - \frac{2}{3}\mu\frac{1}{\epsilon_p}(\nabla \cdot u)I \tag{10}$$

3. Transport of diluted species in porous media.

This set of equations was used to calculate the concentration and transport of the species that move within the fluid that fill (totally or partially) the voids in a solid porous medium and these can be described through convection, diffusion, adsorption, dispersion, and volatilization. In addition to what has already been mentioned, cases are handled in which the solid phase substrate is immobile or when a gas filling medium is immobile. In this case study, the palm shell is considered immobile while the mobile nitrogen, since it diffuses between the pores, is governed by the following equation:

$$\frac{\partial(\epsilon_p c_i)}{\partial t} + \frac{\partial(\rho c_{p,i})}{\partial t} + \nabla .\ J_i + u\ .\ \nabla c_i = R_i + S_i \tag{11}$$

$$J_i = -(D_{D,i} + D_{e,i})\nabla C_i \tag{12}$$

With the transfer phenomena defined, the 2D design of the reactor in COMSOL continues as shown in Figure 2.1 (a), finding results close to those expected in the design, defining the domains and contours in the geometry to find the solutions. Temporal changes of the model, using the "Transport of diluted species in porous media" interface, a kinetic process of isothermal and non-isothermal pyrolysis was carried out to find the operating range of the reaction, adapting the methodology proposed by (Solanki et al., 2022) already with the results that were found, the tubular reactor was scaled to 3 dimensions Figure 2.1 (b), where a cross section was made to carry out the corresponding transfer phenomena, evaluating the 3 equally evident domains.

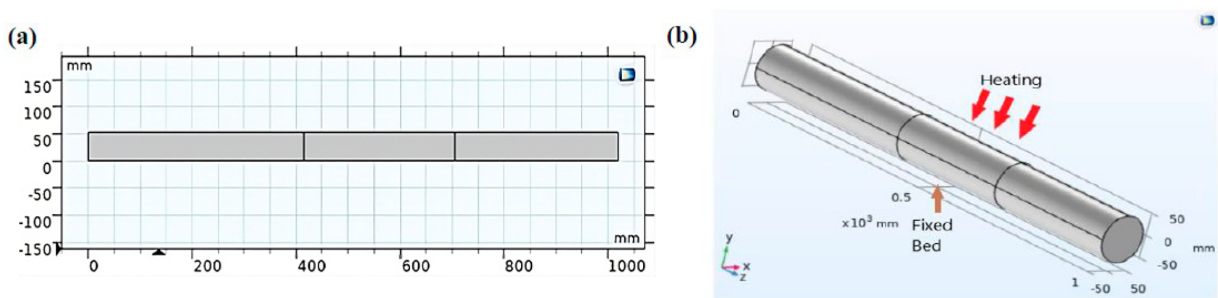

Figure 2.1. Simplified geometric design for the temporary study (a) 2D and (b) 3D.
Note: Own elaboration adapted from Yakub et al. (2015b).

For the isothermal processes, a temperature range was taken from 673.15 to 773.15 K which corresponds to the range where intermediate pyrolysis occurs as mentioned Waluyo et al. (2018) in intervals of 50 K each to determine the temperature range with the maximum reaction rate to obtain tars that were subsequently applied in a non-isothermal process. A non-isothermal process was modelled starting from a dried palm kernel bed at 423.15 K, since this is the maximum temperature for evaporation and drying of water without occurring carbonization of the palm kernel applying the stages described by Sánchez et al. (2017) this reaction was carried out with the heating rate proposed in the operating conditions where after each minute the concentrations of reactants and products were reported at their specific temperature for the time, said process culminated until reaching the optimal temperature range proposed from the isothermal study previously performed.

From the temperature range proposed in the non-isothermal study, the thermal, hydrodynamic profiles and pressure levels were modelled using the mentioned interfaces "Heat transfer in porous media", "Brinkman Equations" and its relation in multiphysics "No isothermal flow" and is governed by the expression , $Qvd=\tau:\nabla u$. Starting from a 2D design to a 3D design of the reactor, the pyrolysis furnaces have a maximum surface temperature operating range of 1573.15 K that corresponds to the reported by Sánchez et al. (2017) and Sechage Cortés et al. (2017) in their laboratory-scale pyrolysis process, the study will be carried out temporarily from the start of the reactor at 650 K and will present an increase of temperature of 30 K for each minute on the surface of the furnace that will be modeled by means of a Dirichlet boundary condition until the process is completed in a time of 17 minutes and a surface temperature of 1160 K, which is within the temperature range mentioned above and reported by the case study of Solanki et al. (2022) where a heating rate of 100 K/min was used up to a surface temperature of 1273.15 K and in this way the thermal profiles, speed magnitudes and pressure levels inside the reactor.

The selected reactor was fixed bed because its operation is simple and with reliable results, taking into account in this study the conduction of the shell within the bed and the gas-solid convection as mentioned (Uddin et al., 2018) facilitating the solution of the mathematical model unlike the fluidized bed where its representation in the software is more complex, with higher computational cost and the number of transfer phenomena present increases (solid-solid conduction) due to the presence of another element that in many studies is sand omitting radiation in both types of reactor.

3. RESULTS AND DISCUSSIONS

3.1. Isothermal and non-isothermal kinetic study

It can be seen in Figure 3 (a), (b) and (c) that pyrolysis comprises favored endothermic reactions in an approximate temperature range of 673.15 to 773.15 K, in the graphs presented it is evident that in isothermal processes there is a primary consumption of hemicellulose followed by lignin and finally cellulose, however biomass is not immediately transformed into the products of interest but into active intermediates by the action of temperature where hemicellulose is the compound with the highest rate of consumption and cellulose together with the active lignin they present a much lower consumption.

In Figure 3 (a) the reaction rate is very slow, reaching a consumption of 40 min with a high production of carbon and non-condensable gases, obtaining a value of 22 mol/m^3 and 9 mol/m^3 of tar with the presence of cellulose and active lignin which can be confirmed with what was stated by Waluyo et al. (2018) since it mentions that in a range of 573.15 to 773.15 K the solids have a high residence time, classifying the process as a slow pyrolysis that not only requires a high energy load but also makes it an inefficient process for the production of tar due to that the long periods of time develop a second cracking that converts the phenolic compounds of the tar into bio-char and gases.

For Figures 3(b) and 3(c) there is an increase in the reaction rate, defining an optimal range to carry out the reaction limited between said temperatures 723.15 and 773.15 K respectively, these data are similar to those evaluated by Kim et al. (2010) where they obtained results of rapid pyrolysis of the palm kernel at different temperatures, mentioning that at 763.15 K the tar production is better and with respect to (Qureshi et al., 2021) optimized the fast pyrolysis process to obtain tar with an operating temperature of 773.15 K.

In turn, to obtain tar, fast pyrolysis should be considered, since at a temperature of 773.15 K in an isothermal process as shown in Figure 3 (c), the reaction occurs after only 300 s, where the production of this liquid takes values of 18 mol/m3 and 11 mol/m3 of bio-char and non-condensable gases, compared to a process at 723.15 K that generates 16 mol/m3 of tar and 18 mol/m3 of bio-char with gases non-condensable in a time of 13 minutes. Biomass in this temperature range presents a higher proportion in phenol tar, acetic acid, furfural, toluene, and phenolic derivatives as presented by Waluyo et al. (2018) and for higher temperatures an instantaneous consumption is observed with the kinetic parameters used in the investigation.

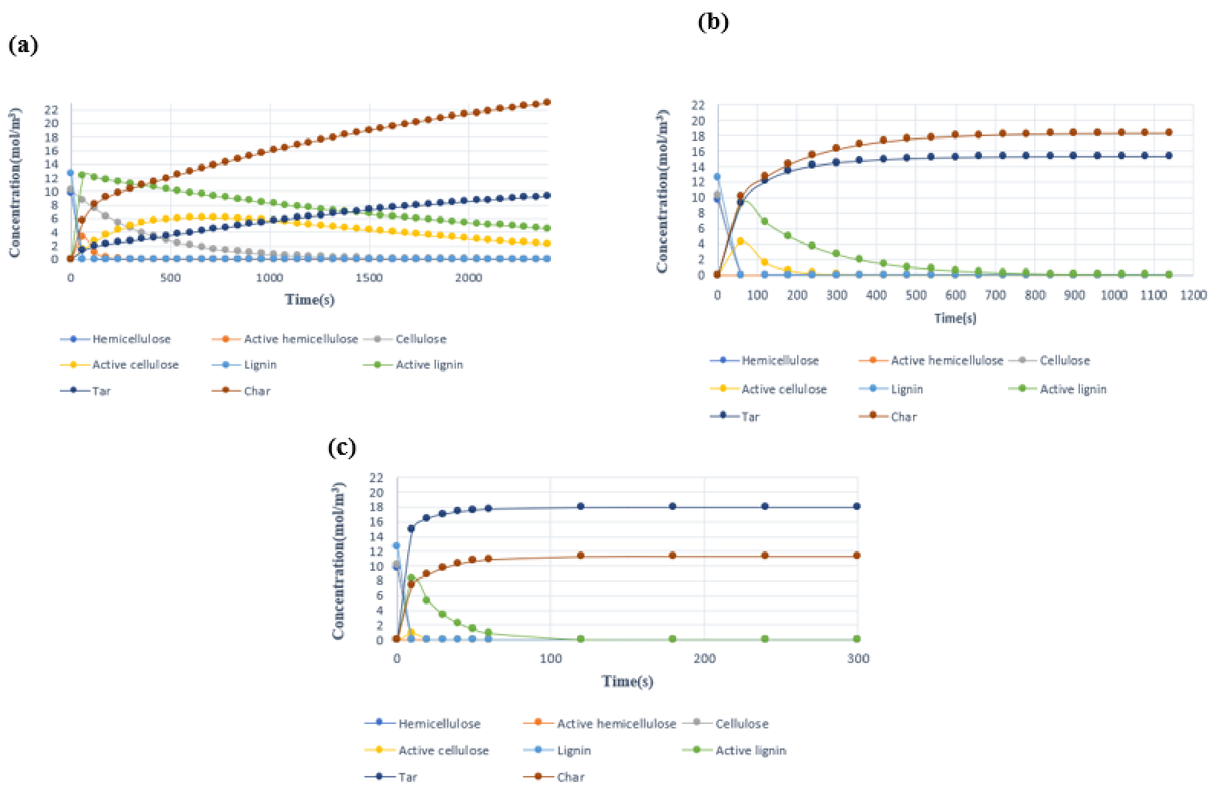

Figure 3. Change in biomass, coal-gas mixture and tar concentration with respect to time at (a) 673.15 K, (b) 723.15 K and (c) 773.15 K.

Figures 4 and 5 show the relationship between concentration and conversion during the non-isothermal pyrolysis process, it is observed that from 423.15 to 623.15 K is the range of consumption of the initial biomass where its conversion reaches the maximum value, in this step the biomass begins to convert into its active components (hemicellulose, cellulose and lignin) which is capable of forming tars or carbon and gases as shown in figure 3, after 623.15 K the production of compounds in organic acids, phenols, compounds phenolics and biochar until reaching 743.15 K, which is equivalent to 11 minutes of reaction where a horizontal asymptote is observed for the pyrolysis products, so the transformation of the biomass does not have considerable changes until the process is completed 15 minutes after it, obtaining 14mol/m^3 of tar and 18 mol/m^3 of biochar and non-condensable gases. This reaction time coincides with that applied by Okoroigwe et al. (2011) where pyrolysis of one kilogram of palm kernel using nitrogen as carrier gas in a range of 723.15 to 773.15 K occurred in a bench screw reactor, culminating after 10 min with a production of 61% w/w of tar, 24% of biocarbon and 15% of non-condensable gases with energy gain with respect to the initial biomass or, the results proposed by Ahmad et al. (2014) who used a reactor of R-303 Series Catatest Reactor System fixed bed loaded with 5 g of palm kernel with a nitrogen gas inlet at 50 mL/min and a heating rate defined at 50 K/min, where after 9 minutes of reaction equivalent to 450 °C, the highest yield of bio-oil was obtained with a maximum value of 38.4% wt, followed by thermal cracking with gas production at 500 °C.

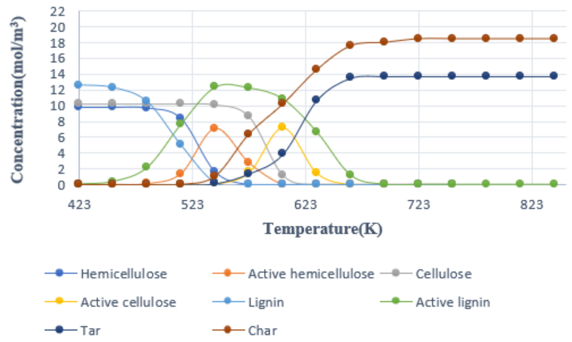

Fig. 4 Change in biomass, coal and tar concentration with respect to temperature

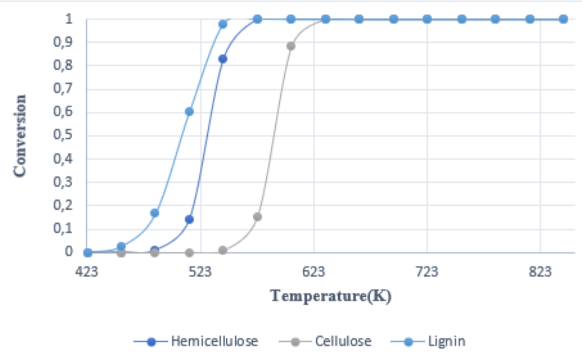

Figure 5. Change in conversion of biomass, coal and tar with respect to temperature.

To carry out a non-isothermal process, the thermal profiles and their variables within the reactor must be guaranteed, the process generates a Biot number greater than 0.1, which informs us that the system suffers from a greater heat transfer by convection than by conduction. for the palm shell, generating problems to be able to condition the fixed bed up to 723.15 K due to the low transfer by conduction.

3.2. Temperature profiles

Figure 6 and 7 show radial isothermal profiles that occur throughout the reactor and the bed when carrying out the pyrolysis process starting from an initial temperature of 423 K in which the shell has low humidity. From these results, denotes a preference in the direction of heat transfer and the average value of the temperature within the bed.

Heat transfer occurs in a radial direction from the reactor surface to the environment in the form of radiation and from the reactor surface to the center of the biomass by means of conduction and convection with slight longitudinal dispersion due to the diameter-to-diameter ratio length, since the value corresponding to the length is higher compared to the radius of the reactor.

For the design of the reactor used, it is evident that with the change in surface temperature there is a linear increase in this variable between the biomass and the nitrogen pumped into the reactor, the latter having a greater impact, the increase in the temperature of the furnace allows the particles of the bed lack a local thermal equilibrium and as a consequence there is a greater transfer of heat in the form of convection from the surrounding nitrogen to the surface of the particles, since having a low flow rate allows a longer residence time flowing between the interstices of the packed bed by increasing the temperature of the particles.

In the same way, through the surface of the particles towards the center of the same by conduction, there is an increase in temperature from the surface of the reactor towards the center of the same as observed in the bed of figure 6, causing that there is a higher average temperature at the edge of the reactor and dissipates to the center, obtaining in a range close to 19 cm from the surface to the center of the biomass, being 0 the surface of the reactor and 52.5 cm the center, an average temperature of 957 K after 17 min, from 19 cm to 32.5 cm an average temperature of 781 K is observed because there is no proximity to the edge of the reactor, from 32.5-42.5 cm with an average temperature of 665 K and 42.5-52.5 with an average temperature of 597.5 K, it is also observed that for biomass there is an average value of 845 K which corresponds to those evaluated in the non-isothermal kinetic study observed in figure 4 where the highest production is obtained. of tar with a complete conversion of the biomass to the products of interest and describes the methodology used by Yakub et al. (2015b)

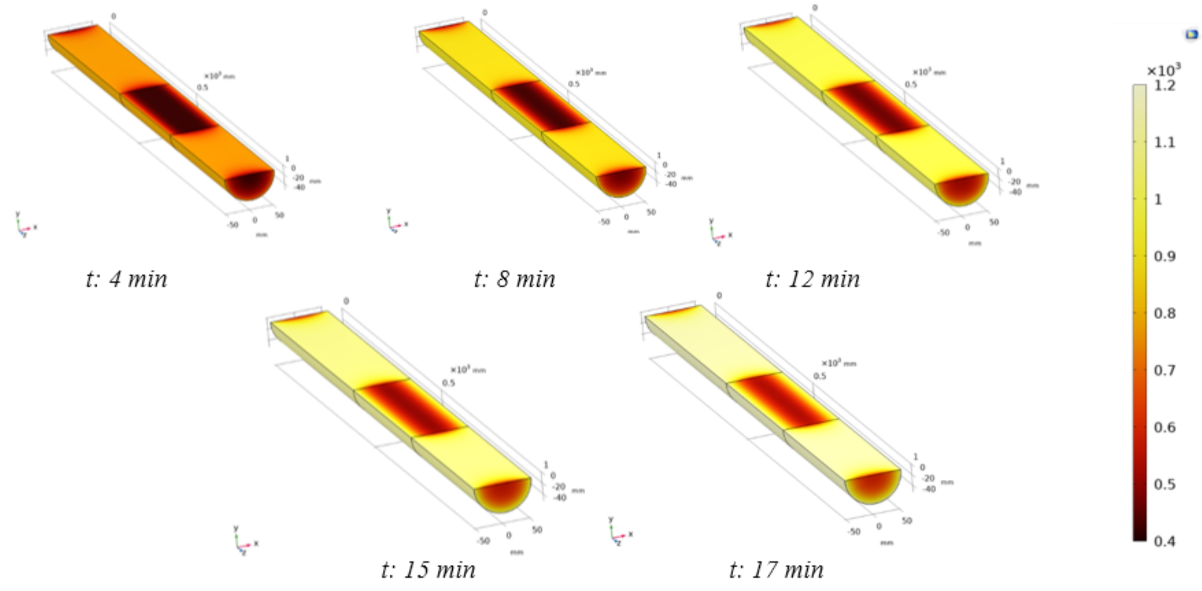

Figure 6. Results of a biomass packed bed over time from 4 to 17 min with a heating rate of 30 K/min.

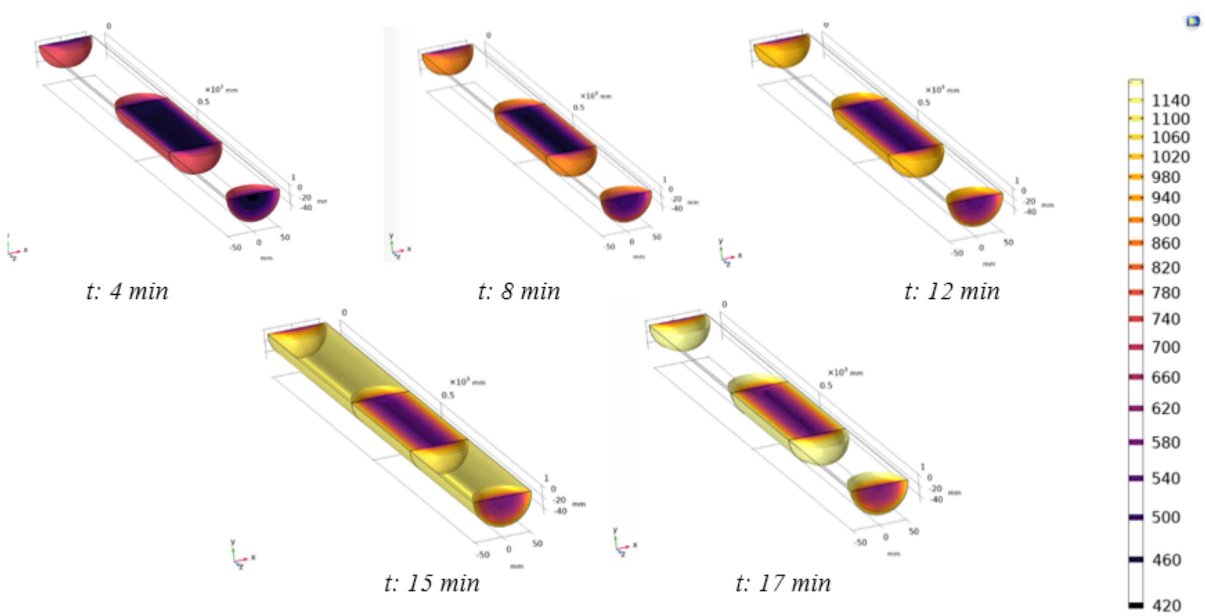

Figure 7. Results in a packed bed of biomass at iso-surface over time from 4 to 17 min with a heating rate of 30 K/min.

3.3 Velocity and pressure profiles

Figure 8 presents the velocity profiles along the reactor for the transfer fluid and its pressure level within the packed bed, nitrogen enters at low velocity, achieving a fully developed flow at the bed inlet and outlet. with laminar state, it is observed in the velocity gradients of figure 8 (a) that the maximum magnitude is located in the center of the reactor with a predominant value at the bed outlet and a drastic loss of it on the surface due to the viscous adherence of the fluid causing a state of rest.

On the other hand, the fluids that pass through a granular medium or cake present variations in the volumetric flow due to the porosity of the bed, the superficial velocity corresponds to the relationship between the incoming flow with the surface area of the geometric body that is manifested as a medium of speed within a porous medium as mentioned Salcedo Díaz & Martin-Gullon (2012).

Figure 8 (a) shows the velocity magnitude for nitrogen with an approximate value of 2.21x10^{-4} m/s, decreasing in proportion as it approaches the edges of the reactor, in the same way the magnitude average gas velocity inside the porous interstices of the bed with a value of 1.16x10^{-4} m/s.

Figure (b) shows that the loss of pressure with respect to the entrance of the fixed bed, this is favored with the increase in speed due to the nature of the fluid that generates spontaneous molecular movements increasing the pressure, in the same way for the fall of pressure ΔP of 287.53 Pa that corresponds to a decrease of 98.7 %, this is a consequence of the circulation flow that, being of very low magnitude, limits the Ergun equation (Salcedo Díaz and Martin-Gullon, 2012) forcing the drop pressure to be directly proportional to the superficial velocity of the bed, which must be taken into account for the design of a pyrolytic process on an industrial scale with gas flow in a laminar state.

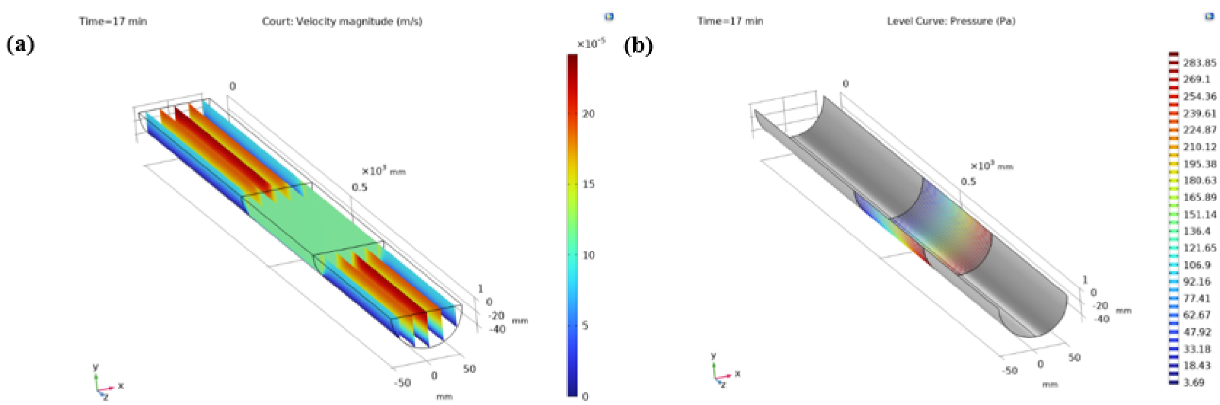

Figure 8. (a) Velocity profile inside the reactor and (b) pressure level at 5.25 cm after 17 min.

4. CONCLUSIONS

The concentrations of tar, biochar and non-condensable gases were determined together with the consumption of the initial biomass, the thermal, hydrodynamic profiles and pressure levels that were produced inside the furnace in a pyrolysis reaction, from these optimum temperature range. internal. was observed in the shell from 723.15 to 773.15 K where the production of highly energetic tar was favored over biochar and gases, in the same way for a non-isothermal discontinuous process with a heating rate of 30 K/min a high concentration can be obtained. of tar with an operation time of 10 to 12 min.

The thermal and hydrodynamic profiles coupled to the proposed reactive system were determined, in which satisfactory average temperatures were observed in a range of 423.15 to 813 K at 12 min of reaction that predict biomass consumption at a heating rate of 30 K /min and its effects on the velocity magnitude for the transfer gas together with its pressure drop in the bed, achieving a maximum velocity in the center of the reactor of 2.16 x10^{-4} m/s, this modeling system with CFD can be applied or extrapolated to an industrial-scale reactor to predict its behavior, operation and optimization.

In addition to this analysis, only the results of a fixed bed reactor were presented by means of CFD, it would be interesting to carry out the study in a fluidized bed reactor, It is recommended that in future research the effect and relationship of the particle size of the biomass entering the reactor with the inert gas velocity and with the heat transfer phenomenon be evaluated, since increasing the size of the material the degradation will take longer and there will be obstruction for the nitrogen that goes through the pores of these particles, as well as changes in properties such as porosity and conductivity will be seen. It is also suggested to use the physical and thermal properties of the palm kernel as functions of temperature and not as constants.

Credit authorship contribution statement

Mariapaz Moreno- Pinilla: Performed the presented simulations, wrote original draft, and presented formal analysis.

Joan Sebastian Rueda- Castiblanco: Performed the simulations presented, Evaluation of the data, drafted the manuscript, and developed the analysis.

Harvey Andres Milquez-Sanabria: Supervision, the simulation and the manuscript.
Jaime Eduardo Arturo-Calvache: Conceptualization, Resources.

Declaration of competing interest

The authors declare that they have no known competing financial interests or personal relationships that could have appeared to influence the work reported in this paper.

5. REFERENCES

Abdullah, N., Sulaiman, F., & Aliasak, Z. (2015). Fast pyrolysis of oil palm shell (OPS). *AIP Conference Proceedings*, *1657*(1), 040008. https://doi.org/10.1063/1.4915169

Ahmad, R., Hamidin, N., Ali, U. F. M., & Abidin, C. Z. A. (2014). Characterization of bio-oil from palm kernel shell pyrolysis. *Journal of Mechanical Engineering and Sciences, 7*(1), 1134–1140. https://doi.org/10.15282/jmes.7.2014.12.0110

Anaya-Aldana, R., and Molina Crespo, D. C. (2018). Economic and financial evaluation of alternatives for the use of raw material residues from an industrial oil palm extraction plant (Evaluación económica y financiera de las alternativas de uso de los residuos de la materia prima de una planta industrial de extracción de palma de aceite). *Dictamen Libre, 1*(22), 81–101. https://doi.org/10.18041/2619-4244/dl.22.5029

Asadullah, M., Ab Rasid, N. S., Kadir, S. A. S. A., & Azdarpour, A. (2013). Production and detailed characterization of bio-oil from fast pyrolysis of palm kernel shell. *Biomass and Bioenergy*, 59, 316–324. https://doi.org/10.1016/j.biombioe.2013.08.037

Ayala-Ruíz, N., Malagón-Romero, D. H., & Milquez-Sanabria, H. A. (2022). Exergoeconomic evaluation of a banana waste pyrolysis plant for biofuel production. *Journal of Cleaner Production*, 359, 132108. https://doi.org/10.1016/j.jclepro.2022.132108

Basu, P. (2018). Chapter 5 - Pyrolysis. In Basu, P. (Ed.) Biomass Gasification, Pyrolysis and Torrefaction (Third Edition, pp. 147-176). Academic Press. https://doi.org/10.1016/B978-0-12-812992-0.00005-4

Castiblanco-Urrego, O., & Milquez-Sanabria, H. A. (2021). Study and simulation of a gasifier with CO2 capture for the production of blue hydrogen from Colombian coal (Estudio y simulación de un gasificador con captura de CO2 para la producción de hidrógeno azul partiendo de carbón colombiano). *Revista UIS Ingenierías, 20*(4), 91–100. https://doi.org/10.18273/revuin.v20n4-2021007

Chang, G., Huang, Y., Xie, J., Yang, H., Liu, H., Yin, X., & Wu, C. (2016). The lignin pyrolysis composition and pyrolysis products of palm kernel shell, wheat straw, and pine sawdust. *Energy Conversion and Management, 124*, 587–597. https://doi.org/10.1016/j.enconman.2016.07.038

Ezeoha, S. L., Akubuo, C. O., & Ani, O. (2012). PROPOSED AVERAGE VALUES OF SOME ENGINEERING PROPERTIES OF PALM KERNELS. *Nigerian Journal of Technology (NIJOTECH), 31*(2), 167–173. https://www.nijotech.com/index.php/nijotech/article/view/10

Fedepalma. (2021). Oil palm in Colombia (La palma de aceite en Colombia). https://publicaciones.fedepalma.org/index.php/anuario/article/view/13235/13024.

Hussain, M., Zabiri, H., Tufa, L. D., Yusup, S., & Ali, I. (2022). A kinetic study and thermal decomposition characteristics of palm kernel shell using model-fitting and model-free methods. *Biofuels, 13*(1), 105–116. https://doi.org/10.1080/17597269.2019.1642642

Kim, S. J., Jung, S. H., & Kim, J. S. (2010). Fast pyrolysis of palm kernel shells: Influence of operation parameters on the bio-oil yield and the yield of phenol and phenolic compounds. *Bioresource Technology*, *101*(23), 9294–9300. https://doi.org/10.1016/j.biortech.2010.06.110

Fono-Tamo, R. S., & Koya, O. A. (2013). Characterization of pulverised palm kernel shell for sustainable waste diversification. *International Journal of Scientific and Engineering Research*, *4*(4), 43-50.

Liu, B., Papadikis, K., Gu, S., Fidalgo, B., Longhurst, P., Li, Z., & Kolios, A. (2017). CFD modeling of particle shrinkage in a fluidized bed for biomass fast pyrolysis with quadrature method of moment. *Fuel Processing Technology, 164*, 51–68. https://doi.org/10.1016/j.fuproc.2017.04.012

Ministry for the ecological transition. (2020) *ENERGY RECOVERY / THERMAL TREATMENTS. (VALORIZACIÓN ENERGÉTICA / TRATAMIENTOS TÉRMICOS)*. https://www.miteco.gob.es/en/calidad-y-evaluacion-ambiental/temas/prevencion-y-gestion-residuos/flujos/domesticos/gestion/sistema-tratamiento/Incineracion.aspx

Okoroigwe, E. C., Li, Z., Godwin Unachukwu, Stuecken, T., & Saffron, C. (2011). Thermochemical conversion of Palm Kernel Shell (PKS) to bio-energy. ASME 2011 5th International Conference On Energy Sustainability, Parts A, B, And C, 1183-1191. http://doi.org/10.1115/ES2011-54690

Okoye, N. M., Nnaemeka Madubuike, C., Uba Nwuba, I., Orakwe, L. C., & Ugwuishiwu, O. B. 2018. Computational Fluid Dynamics Modeling of Residence Time Distribution in a Field-Scale Horizontal Subsurface Flow Constructed Wetland with Palm Kernel Shell as Substrate. World Scientific News, (109), 60-70.

Pauls, J. H., Mahinpey, N., & Mostafavi, E. (2016). Simulation of air-steam gasification of woody biomass in a bubbling fluidized bed using Aspen Plus: A comprehensive model including pyrolysis, hydrodynamics and tar production. *Biomass and Bioenergy, 95,* 157–166. https://doi.org/10.1016/j.biombioe.2016.10.002

Qureshi, K. M., Kay Lup, A. N., Khan, S., Abnisa, F., & Wan Daud, W. M. A. (2021). Optimization of palm shell pyrolysis parameters in helical screw fluidized bed reactor: Effect of particle size, pyrolysis time and vapor residence time. Cleaner Engineering and Technology, 4, 100174. https://doi.org/10.1016/j.clet.2021.100174

Ramanathan, A., Begum, K. M. M. S., Pereira, A. O., & Cohen, C. (2022). Chapter 2 - Biomass pyrolysis system based on life cycle assessment and Aspen plus analysis and kinetic modeling. In Ramanathan, A., Begum, K. M. M. S., Pereira, A. O., & Cohen, C. (Eds.), *A Thermo-Economic Approach to Energy From Waste* (pp. 35–71). Elsevier. https://doi.org/10.1016/B978-0-12-824357-2.00006-1

Reyes Rodriguez, D. A., Reyes Trejos, O. Y., & Camargo Vargas, G. de J. (2019). Evaluation of the pyrolysis and co-pyrolysis process of palm shell and waste tyres in a co2 atmosphere. Avances Investigación En Ingeniería, 16(2), 83-92. https://doi.org/10.18041/1794-4953/avances.2.5501

Salcedo Díaz, R., & Martin-Gullon, I. (2012). *Materials of the subject Fluid Mechanics (Materiales de la asignatura Mecánica de Fluidos)*. Capítulo 4, 1–50. http://rua.ua.es/dspace/handle/10045/20299

Sánchez Alfonso, R. A., Duran Peralta, H. A., Aguiar Urriago, L. M., Uribe Aldana, N., & Rojas Forero, A. Y. V. (2018). Model for the Gasification of the Oil Palm Kernel Shell (Modelo para la gasificación del cuesco de palma aceitera). *Ingenium, 18*(36), 81–100. https://doi.org/10.21500/01247492.3433

Sechage Cortés, J. S., Gómez Sandoval, D. L., Rodríguez Meléndez, A. G., & Mayorga Betancourt, M. A. (2017). Mathematical Modelingfor the Pyrolysis of the Oil Palm Kernel Shell (Modelamiento matemático para la pirolisis del cuesco de palma aceitera). *Ingenium, 18*(36), 44–56. https://doi.org/10.21500/01247492.3430

Solanki, S., Baruah, B., & Tiwari, P. (2022). Modeling and simulation of wood pyrolysis process using COMSOL Multiphysics. *Bioresource Technology Reports, 17*. https://doi.org/10.1016/j.biteb.2021.100941

Thoharudin, N., Chen, Y., & Hsiau, S. (2020). Numerical Studies on Fast Pyrolysis of Palm Kernel Shell in a Fluidized Bed Reactor. *IOP Conference Series Materials Science And Engineering, 874*(1), 012033. https://doi.org/10.1088/1757-899x/874/1/012033

Tripathi, M., Sahu, J. N., Ganesan, P., & Jewaratnam, J. (2016). Thermophysical characterization of oil palm shell (OPS) and OPS char synthesized by the microwave pyrolysis of OPS. *Applied Thermal Engineering, 105*, 605–612. https://doi.org/10.1016/j.applthermaleng.2016.03.053

Uddin, M.N., Techato, K,; Taweekun, J., Rahman, M.M., Rasul, M.G., Mahlia, T.M.I., & Ashrafur, S.M. (2018). An Overview of Recent Developments in Biomass Pyrolysis Technologies. *Energies, 11*, 3115. https://doi.org/10.3390/en11113115

Van Dam, J. (2016). Oil Palm By-Products as Biomass Commodities (Subproductos de la palma de aceite como materias primas de biomasa). *Palmas, 37*, 149-156.

Verdeza-Villalobos, A., Lenis-Rodas, Y. A., Bula-Silvera, A. J., Mendoza-Fandiño, J. M., & Gómez-Vásquez, R. D. (2019). Performance analysis of a commercial fixed bed downdraft gasifier using palm kernel shells. *CTyF - Ciencia, Tecnologia y Futuro, 9*(2), 79–88. https://doi.org/10.29047/01225383.181

Waluyo, J., Makertihartha, I. G. B. N., & Susanto, H. (2018). Pyrolysis with intermediate heating rate of palm kernel shells: Effect temperature and catalyst on product distribution. *AIP Conference Proceedings, 1977(*1), 020026. https://doi.org/10.1063/1.5042882

Wijayanti, W., Musyaroh, Sasongko, M. N., Kusumastuti, R., & Sasmoko. (2021). Modelling analysis of pyrolysis process with thermal effects by using Comsol Multiphysics. *Case Studies in Thermal Engineering, 28*, 101625 https://doi.org/10.1016/j.csite.2021.101625

Yakub, M., Abakr, Y. A., Kazi, F. K., Yusuf, S., Alshareef, I., & Chin, S. A. (2015a). Pyrolysis of Napier grass in a fixed bed reactor: Effect of operating conditions on product yields and characteristics. *BioResources. 10*(4), 6457-6478.

Yakub, M. I., Abdalla, A. Y., Feroz, K. K., Suzana, Y., Ibraheem, A., & Chin, S. A. (2015b). Pyrolysis of Oil Palm Residues in a Fixed Bed Tubular Reactor. *Journal of Power and Energy Engineering, 03*(04), 185–193. https://doi.org/10.4236/jpee.2015.34026

Notations

A_i – Pre-exponential factor s− ¹ ,

$C_{p,b}$ – Dry bulk heat capacity at constant pressure J/(kg·K)

$C_{p,f}$ – Specific heat capacity at constant pressure, fluid phase J/(kg·K)

$C_{p,imf}$ – Specific heat capacity at constant pressure of immobile fluid in porous media J/(kg·K)

$C_{p,s}$ – Specific heat capacity at constant pressure, solid phase J/(kg·K)

∇C_i – Concentration gradient by species i mol/m^4

$D_{D,i}$ – Dispersion tensor by species i m^2 /s

$D_{e,i}$ – Effective diffusion coefficient for species i m^2 /s

Ea_i – Activation energy J/mol

F – Force kg/m^{2}s^2

J_i – Flow of species i mol/m^{2}s

K – Permeability of the porous medium m^2

K_b – Dry bulk thermal conductivity W/(m·K)

K_{disp} – Dispersive thermal conductivity tensor W/(m·K)

K_{eff} – Effective thermal conductivity W/(m·K)

K_f – Thermal conductivity, fluid phase W/(m·K)

k_i – Reaction rate constant i s

K_{imf} – Effective thermal conductivity W/(m·K)

K_s – Thermal conductivity, solid phase W/(m·K)

K_p – Thermal conductivity in porous medium W/(m·K)

q – Conductive heat flux W/m^2

q – Radiative heat flux W/m^2

Q – Heat source / Heat sink W/m^2

q_0 – Inward heat flux W/m^2

Q_{geo} – Geothermal heat source W/m^3

Q_m – mass source or sink kg/(m^{3}s)

Q_p – Pressure work W/m^3

Q_{vd} – Viscous dissipation W/ (m· K)

S_i – Unit vector of discrete direction in space, i-th component

∇T – Temperature gradient K/m

R – Gas constant J/(mol· K)

T – Temperature K

t – Time min

u – Velocity m/s

Greek letters

ρ_f – Density, fluid phase kg/m^3

ρ_{imf} – Density of immobile fluid in porous media kg/m^3

ρ_s – Density of solid material kg/m^3

ρ_b – Dry bulk density kg/m^3

β – Parameter used for the Ergun equation 1/m

τ – Viscous stress tensor Pa

μ – Dynamic viscosity Pa·s

ϵ_p –Porosity

ε –Emissivity

θ_{imf} – Volume fraction of immobile fluid in porous media

θ_p – Volume fraction

θ_s – Volume fraction of solid material in porous media and fractures

σ –Stefan's constant

Subscripts

amb– Ambient

c – Cellulose

f– Fluid

h – Hemicellulose

i – Common index of component or phase

imf- Immobile fluid

j – Common index of component or phase

l – Lignin

s – Solid